

Changes in the electrical resistivity of amorphous Ni-Zr alloy during the initial stages of crystallization

G. E. Abrosimova, A. S. Aronin, V. F. Gantmakher, Yu. B. Levin, and M. V. Osherov

Institute of Solid-State Physics, Academy of Sciences of the USSR, Chernogolovka, Moscow Province

(Submitted December 31, 1987)

Fiz. Tverd. Tela (Leningrad) 30, 1424-1430 (May 1988)

It was found that crystallization of an amorphous alloy of the composition NiZr_x reduced the resistivity, but this was preceded by a 4-5% increase in the resistivity. Possible causes of such an increase due to spatial inhomogeneities were considered, including boundaries between amorphous and crystalline regions and large-scale fluctuations of the composition of the amorphous matrix at the onset of crystallization. This consideration was based on the experimental data for the parameters of a metastable crystalline phase (unit-cell constants, space group, and chemical composition) and on the nature of the superconducting transition (broadening of the transition in the samples in which crystallization occurred only in a small fraction of the total volume).

Amorphous alloys of transition metals exhibit a high resistivity ρ corresponding to a mean free path of carriers ℓ of the order of the interatomic space a . Crystallization usually increases ℓ and reduces the resistivity ρ . However, this is not always that simple. Frequently, the process of crystallization results in more complex changes in ρ : a rise precedes a fall of the resistivity. A study of such a complex dependence can provide data on the crystallization kinetics. Moreover, measurements of the electrical resistivity can identify accurately the various stages of the crystallization process.

One can approach changes in the resistivity during crystallization also from a different point of view. There have been thorough studies of the electrical resistivity of a crystalline metal in which the disturbances of the periodicity in the distribution of atoms are small and can be regarded as perturbations. It is natural to consider the influence of nuclei of the ordering in an amorphous matrix on the resistivity.

We investigated the maximum of the resistivity observed at the onset of crystallization in the case of an alloy of the Ni_{0.34}Zr_{0.66} composition. Electrical properties of amorphous alloys belonging to the Ni-Zr system have been investigated sufficiently thoroughly in a wide range of concentrations.^{1,2} The alloys with high Zr concentrations are nonmagnetic and exhibit a superconducting transition. The temperature coefficient of the resistivity of these alloys is negative. Some investigations have been made of the density of electron states in these alloys.³ Studies have been made and descriptions have been provided of the influence of structural relaxation on electrical (particularly superconducting^{4,5}) and thermal^{6,7} properties. Several studies have also been made^{8,11} of the crystallization of these amorphous alloys in which formation of metastable phases occurs during the initial stages of the process. A phase has been observed with a body-centered tetragonal lattice characterized by the parameters $a = 0.647$ nm and $c = 0.524$ nm (Ref. 8), a phase with a simple cubic lattice and $a = 1.21$ nm (Ref. 9), and others.

All this makes the Ni-Zr alloys convenient materials for an investigation of this kind.

1. Experiments

An amorphous ribbon of Ni_xZr_{1-x}, formed

by quenching a melt on a rapidly rotating copper ring, had the following parameters: $x = 0.34$, $\rho_{300} = 168 \mu\Omega \cdot \text{cm}$, $\rho_{4.2}/\rho_{300} = 1.057$, and density $d = 7.06 \text{ g/cm}^3$. The superconducting transition temperature in the original ribbon was 2.45 K, which was slightly less than the average value.¹² The width of the superconducting transition was 4-8 mK, which was close to the theoretical limit set by fluctuations.^{4,13} Since the dependence of T_C on the nickel concentration x was characterized by the derivative $\partial T/\partial x = 8.5 \text{ K/x}$ (Ref. 1), the relative inhomogeneity of the composition of the sample $\Delta x/x$ averaged over distances of the order of the coherence length $\xi \approx 10^{-5} - 10^{-6} \text{ cm}$ did not exceed 1%.

Samples of the ribbon of 1×10 mm dimensions with four nickel-wire pressure contacts could be cooled to helium temperatures and without altering the mounting assembly they could be also heated in oil-free 10^{-7} Torr vacuum to 1000°C. The rate of change of temperature could be varied within wide limits. The electrical resistivity was measured under dc conditions.

The continuous curve in Fig. 1 represents a typical change in the resistivity during heating of a sample. The lower part of the curve, representing a plateau after completion of the crystallization process, is not included in the figure. We can see that near the crystallization temperature $T_X \approx 400^\circ\text{C}$ the resistivity of the crystalline phase was 1.3 times less than that of the amorphous phase, amounting to about $125 \mu\Omega \cdot \text{cm}$. Cooling of the crystalline phase to 4.2 K reduced the resistivity to $65 \mu\Omega \cdot \text{cm}$, so that the difference was a factor of 3.

The maximum shown in Fig. 1 could be observed only if the heating was sufficiently slow. In the case of the curves shown in Fig. 1 the rise took 20 min and the subsequent crystallization about 1 h. Such a slow crystallization process made it possible to interrupt it at any moment by switching off the heat source. The temperature dependences of the resistivity obtained by cooling during various stages of the crystallization process were also determined (dashed curves in Fig. 1). Low-temperature electrical measurements were followed by x-ray diffraction and electron-microscopic examinations, which made it possible to determine the volume of the crystalline phase and its composition. The x-ray struc-

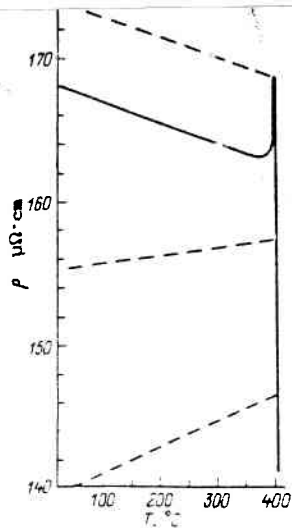


FIG. 1. Changes in the resistivity of $\text{Ni}_{0.34}\text{Zr}_{0.66}$ on increase in temperature. The dashed lines represent the resistivity measured during cooling after interruption of the crystallization process at various stages.

ture analysis was made by the Debye-Scherrer method and diffractometry. Foils needed in electron microscopy were prepared by thinning with an ion beam. The density of the alloys was measured by hydrostatic weighing.

2. Experimental Results

Heat treatment of an amorphous alloy of the investigated composition at temperatures $T \sim 200\text{--}350^\circ\text{C} < T_x$ did not cause crystallization¹⁴ but nevertheless altered the electrical resistivity to the extent of $\Delta\rho/\rho \approx 0.1\text{--}0.01\%$. We ignored such small changes and concentrated our attention on changes which were of the order of the maximum, i.e., which amounted to a few percent.

Subject to this comment, we shall now summarize the results which should be considered in discussing the nature of the maximum of the dependence $\rho(T)$.

1) Deviation of $\rho(T)$ from linearity near 385°C was due to the onset of crystallization. In principle, the crystalline phase could also result from prolonged heat treatment at low temperatures.¹⁵ However, until the beginning of rise of the resistivity the amount of the crystalline phase (if it appeared at all) was too low to detect by diffraction methods (the sensitivity of which was of the order of 0.5%).

2) Cooling from the $\rho = \rho_{\text{max}}$ state did not alter the initial change in the resistivity by $\Delta\rho/\rho \approx 4\text{--}5\%$ and this was true right down to helium temperature.

3) In the $\rho = \rho_{\text{max}}$ state the volume of the crystalline phase was about 10-15%. This range was the scatter for different samples. Figure 2 is a photomicrograph of a part of one of the samples quenched from the maximum of the $\rho(T)$ curve. It shows crystallites of the order of 100 nm in the amorphous matrix. The conditions during recording of this photograph were such that crystallites of size down to 2 nm could be detected. It is clear from Fig. 2 that crystallization did not result in the formation of a large number of small grains in the amorphous matrix.

4) Figure 3 shows the results of a study of the superconducting transition in one of the samples

after different heat treatments. Heating corresponding to the linear part of the dependence $\rho(T)$ shifted the superconducting transition, but it still remained narrow (3-4 mK). In the $\rho = \rho_{\text{max}}$ state the transition was considerably broadened. At the end of the crystallization process the transition became as narrow as initially, but the position shifted too $T_c = 1.46$ K.

5) We determined the parameters of the crystalline phase. It had a metastable orthorhombic lattice, not observed before and characterized by the following parameters: $a = 0.904 \pm 0.005$, $b = 0.445 \pm 0.010$, $c = 0.400 \pm 0.005$ nm. The space group was $P2_12_12_1$; it was deduced from the reflections in point-like electron diffraction patterns in accordance with the general extinction rules.^{16,17} The relatively large error in the determination of the unit cell parameters was due to two factors. Firstly, the error was increased by the complex internal structure of the crystallites (Fig. 2) and by stresses, which made the lines in the x-diffractograms fairly wide. Secondly, the positions of these lines depended (though weakly) on the crystallization stage. This was probably due to a change in the degree of nonstoichiometry in the crystalline phase. It should be pointed out that we did not observe the equilibrium phase of NiZr_2 or the metastable phases described in Refs. 8-11.

Since the crystalline part of the sample consisted of a single phase when at least 60% of the sample was crystallized, the concentration of nickel in the crystalline phase was within the range $0.23 \leq x \leq 0.45$. The values of the density and of the lattice parameters could be used to find the number of atoms in a unit cell. This number was 8, provided the concentration of zirconium was high ($x \approx 0.23$), or it was 9 when the concentration of nickel was high ($x \approx 0.45$).

3. Discussion of Results

Crystallization is sometimes preceded by a new state characterized by chemical ordering. It is possible that the observed increase in the resistivity is due to this chemical ordering. This would be particularly interesting because a state with a high resistivity could be frozen (Fig. 1). However, the available experimental data were insufficient to confirm this hypothesis. We therefore considered al-

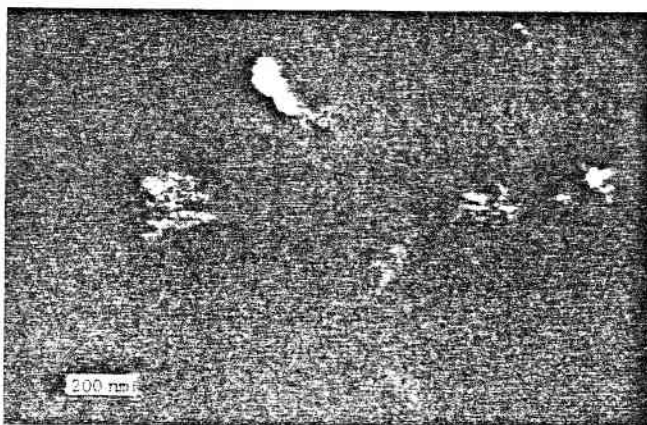


FIG. 2. Structure of an alloy quenched from a temperature corresponding to the maximum value of the resistivity.

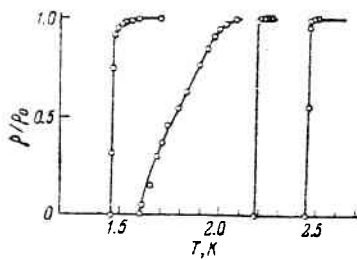


FIG. 3. Superconducting transition in an amorphous film in the initial state and after different heat treatments.

ternative explanations of the rise of the resistivity due to the appearance of crystalline inclusions. Two factors could be important: the resistivity of the boundaries between amorphous and crystalline materials and the appearance of large-scale fluctuations of the concentration in the amorphous phase because the chemical composition of the crystalline phase differed from that of the amorphous matrix. We shall now consider these two factors.

Resistivity of the boundaries

If we use expressions from the theory of an effective medium¹⁸ for the electrical resistivity ρ of a random mixture of two media with the conductivities $\sigma_1 = 1/\rho_1$ (amorphous phase) and $\sigma_2 = 1/\rho_2$ (crystalline phase), we find that the dependence of ρ/ρ_1 on the concentration p_2 of the crystalline phase is described by the lower curve in Fig. 4. In fact, this curve differs little from a straight line.

We shall now consider the other limiting case when the boundaries between the phases are completely impermeable to an electric current. Then, the appearance of isolated crystalline inclusions in the amorphous matrix first reduces the effective cross section of the conductor and increases ρ . This increase continues until the concentration of the crystalline phase p_2 reaches the percolation threshold $p_c \approx 0.15$, when percolation begins in the crystalline phase. If $p_2 > p_c$, the current flows along two independent conductors connected in parallel: one is amorphous and the other crystalline. Finally, in the range $p_2 > 1 - p_c$ the residue of the amorphous phase increases the effective resistivity of the crystalline conductor.

Numerical experiments on the conductivity of metallic inclusions in an insulating matrix¹⁹ indicate that the conductivity of each phase can be described by the following expression.

$$\sigma/\sigma_0 = \begin{cases} 0, & p < 0.15 \\ 1.44(p - 0.15)^{1.6}, & 0.15 < p < 0.6, \\ 0.5(3p - 1) & 0.6 < p, \end{cases} \quad (1)$$

where σ_0 is the conductivity of a given phase and p is its concentration. The expressions in Eq. (1) are based on the generally accepted values of the percolation threshold $p_c = 0.15$ for a three-dimensional system and of the exponent 1.6 in the power law, and also on the expression for $\sigma(p)$ obtained in the theory of an effective medium at high values of p . Assuming that the conductivities of the two phases are related by $\sigma_2 = 1.3\sigma_1$ and the concentrations obey the obvious expressions $p_2 = 1 - p_1$, we find that ρ/ρ_1 is described by the upper curve in Fig. 4.

When the resistivity of a boundary varies from

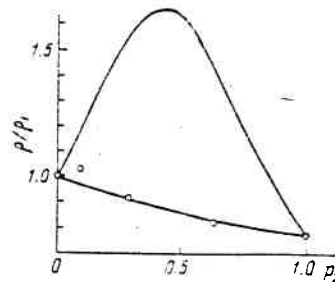


FIG. 4. Resistivity of a ribbon plotted as a function of the proportion of the crystalline phase. The continuous curves are obtained by approximating the effective phase in the two limiting assumptions about the phase boundary (see text).

zero to ∞ , the dependence of ρ/ρ_1 on p shifts from the lower to the upper curve. Points plotted in Fig. 4 are based on the measurements of the concentration of the crystalline phase deduced from photomicrographs of the type shown in Fig. 2. Such measurements are not very accurate. However, it is important that the maximum of $\rho(T)$ occurs at concentrations p_2 close to the percolation threshold p_c .

We shall introduce the probability that an electron crosses the boundary between the crystalline and amorphous phases and we shall select a layer of thickness l containing this boundary (Fig. 5). Then, the resistance of a boundary can be estimated as follows (see Ref. 19). The current J flowing across a boundary of area S is

$$J = nev_{dr}S = ne \frac{eV}{\hbar k_F} S, \quad (2)$$

where n is the carrier density; k_F is the Fermi wave vector; V is the voltage drop across a layer of thickness l ; the drift velocity is v_{dr} and it is due to an electron energy $v_{dr}\hbar k_F = eV$ acquired as a result of crossing the layer in question. Therefore, the resistance of a slab of length L containing a single boundary is

$$R = \frac{\hbar k_F}{ne^2 l} \frac{L-l}{S} + \frac{1}{2} \frac{\hbar k_F}{n^2} \frac{1}{S} = \frac{1}{S} \frac{\hbar k_F}{ne^2} \left(\frac{L}{l} + \frac{1-l}{2} \right). \quad (3)$$

We do not know of any rigorous calculations of the contribution made to the resistance by a single boundary. However, such a calculation has been carried out for the phonon thermal conductivity.²⁰ Using the analogy between the thermal and electrical conductivities, we can find the contribution to the resistance made by a single boundary and we find that the result is typical of that given above.

The length L in Eq. (3) is the average distance between the boundaries. We can estimate L on the assumption that the crystalline phase is in the form of little spheres of diameter d and the concentration of this phase is $Nd^3 = p$. Then, L can be determined from the total cross-sectional area Σ of these spheres per unit volume: $L = \Sigma^{-1} = (Nd^2)^{-1} =$

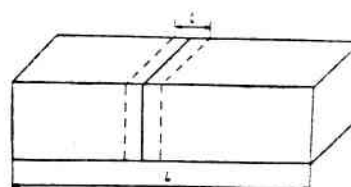


FIG. 5. Single phase boundary.

d/p_2 , and the final expression for the resistivity is

$$\rho = \frac{\hbar k_F}{\pi e^2} \left(\frac{1}{p_2} \frac{d}{l} + \frac{1-\alpha}{\alpha} \right) \frac{p_2}{d} = \frac{\hbar k_F}{\pi e^2 l} \left[1 + \frac{p_2 l (1-\alpha)}{\alpha d} \right]. \quad (4)$$

If we assume that $p_2 = 0.1$ and $l = 10 \text{ \AA}$, the experimentally determined size of crystallites $d \sim 5 \cdot 10^{-5} \text{ cm}$ and the relative magnitude of the maximum $\Delta\rho/\rho \approx 0.05$ yield $\alpha \approx 0.02$.

There are as yet no theoretical models which could be used to compare with this value. Moreover, we cannot say anything about the thickness of the boundary, which is introduced in a purely phenomenological manner. This are some grounds for assuming that the resistivity may be due to the contact between disordered and ordered phases. Then the boundary reduces to a barrier of atomic width and α is the permeability of this barrier. However, we can easily see that the boundary may be much wider. Near the crystallization front we can expect, in principle, strong deviations of the concentrations of the components of the alloy from the average values and an increase in the impurity concentration.

This analysis is valid as long as the thickness of an inhomogeneous layer is much less than the size of crystallites. If this is not true, then the second factor is of importance and we shall now consider it in detail.

Disturbance of the concentration homogeneity of the amorphous phase

According to the data of Ref. 1, an increase in the Ni concentration near the value $x_0 = 0.34$ of interest to us increases the resistivity of amorphous $\text{Ni}_x\text{Zr}_{1-x}$ alloys and reduces T_C . Therefore, we can try to explain the rise of the resistivity to ρ_{max} and a simultaneous broadening of the superconducting transition toward lower temperatures by the appearance of nickel-rich regions in the amorphous matrix.

Using the equation from the theory of an effective medium¹⁸ to describe the average conductivity σ_m

$$\int d\sigma_f \frac{\sigma - \sigma_m}{\sigma + 2\sigma_m} = 0, \quad (5)$$

and assuming that the distribution function f_0 is exponential

$$f_0 = \lambda_0 \exp[-\lambda_0(x - 0.34)], \quad 0 \leq x \leq 1 \quad (6)$$

(the unit conductivity is that of an amorphous alloy with $x = x_0 = 0.34$), we find from the experimental value $\sigma_m = 0.95$ that the variance is $\lambda_0 = 20$. Taking from Ref. 1 the derivatives $\partial\sigma/\partial x$ and $\partial T_C/\partial x$ [$t(x) = T_C(x)/T_C(0.34)$], we can use λ_0 to find the variance of the concentration λ_x and of the temperature of the superconducting transition λ_T . The last quantity shows that at $T = 1.6 \text{ K}$, when the resistivity of a sample falls to zero, the proportion of superconducting regions is $q = 0.38$. It follows from Eq. (1) that the effective cross section of an infinite superconducting cluster is then 0.14. This is a reasonable values.

The situation is not as satisfactory in the case of the variance of the concentrations. The value of λ_x shows that the average \bar{x} in the amorphous part of the of the sample decreases by 0.1, i.e., to 0.44. This cannot be true because the volume

of the crystalline phase is small and such an excess of nickel cannot be established. It is natural to assume that the variable of the conductivity is not only due to concentration gradients, but also due to other factors. However, such complications of the model make it much less attractive.

It thus follows that none of the models can account fully for the experimental observations. The hypothesis that the additional resistivity is concentrated at the boundary does not agree with the broadening of the superconducting transition. If we assume that the amorphous phase is inhomogeneous, we find that the concentration gradients would have to be unrealistically high. It is possible that the results obtained are due to some combination of these factors. Further studies of this alloy are therefore needed and one should also look for other materials where the situation might be simpler.

The authors are grateful to I. A. Voropanova for technical help, and to E. A. Brener and A. V. Serebryakov for valuable discussions.

- ¹Z. Altounian and J. O. Strom-Olsen, Phys. Rev. B **27**, 4149 (1983).
- ²M. Tenhover and W. L. Johnson, Phys. Rev. B **27**, 1610 (1983).
- ³J. -M. Mariot, C. F. Hague, P. Oelhafen, and H. J. Güntherodt, J. Phys. F. **16**, 1197 (1986).
- ⁴S. J. Poon, Phys. Rev. B **27**, 5519 (1983).
- ⁵A. Inoue, K. Matsuzaki, N. Toyota, H. S. Chen, T. Masumoto, and T. Fukase, J. Mater. Sci. **20**, 2323 (1985).
- ⁶D. M. Kroeger, C. C. Koch, J. O. Scarbrough, and C. G. McKamey, Phys. Rev. B **29**, 1199 (1984); J. Non-Cryst. Solids **61-62**, 937 (1984).
- ⁷H. W. Gronert, D. M. Herlach, A. Sröder, R. van den Berg, and H. von Zohnen, Z. Phys. B **63**, 173 (1986).
- ⁸G. K. Dev and S. Banerjee, in: Rapidly Quenched Metals (Proc. Fifth Intern. Conf., Würzburg, West Germany, 1984, ed. by S. Steeb and H. Warlimont), Vol. 1, North-Holland, Amsterdam (1985), p. 343.
- ⁹Z. Altounian, E. Batalla, J. O. Strom-Olsen, and J. L. Walter, J. Appl. Phys. **61**, 149 (1987).
- ¹⁰D. S. Easton, C. G. McKamey, D. M. Kroeger, and O. B. Savin, J. Mater. Sci. **21**, 1275 (1986).
- ¹¹C. G. McKamey, D. M. Kroeger, D. S. Easton, and J. O. Scarbrough, J. Mater. Sci. **21**, 3863 (1986).
- ¹²Q. Zhang, H. U. Krebs, and H. C. Freyhardt, in: Rapidly Quenched Metals (Proc. Fifth Intern. Conf., Würzburg, West Germany, 1984, ed. by S. Steeb and H. Warlimont), Vol. 1, North-Holland, Amsterdam (1985), p. 707.
- ¹³S. J. Poon and P. L. Dann, J. Low Temp. Phys. **54**, 81 (1984).
- ¹⁴J. Hillairet, E. Balanzat, N. Derradji, and A. Chamberod, J. Non-Cryst. Solids **61-62**, 781 (1984).
- ¹⁵M. Thomas, M. G. Scott, and R. W. Cahn, in: Rapidly Quenched Metals (Proc. Fifth Intern. Conf., Würzburg, West Germany, 1984, ed. by S. Steeb and H. Warlimont), Vol. 1, North-Holland, Amsterdam (1985), p. 739.
- ¹⁶C. Lonsdale (ed.), International Tables for X-Ray Crystallography, Vol. 1, Kynoch Press (1952).
- ¹⁷G. Zhdanov and V. Pospelov, Zh. Éksp. Teor. Fiz. **15**, 709 (1945).
- ¹⁸S. Kirkpatrick, Rev. Mod. Phys. **45**, 574 (1973).
- ¹⁹Yu. V. Sharvin, Zh. Éksp. Teor. Fiz. **48**, 984 (1965) [Sov. Phys. JETP **21**, 655 (1965)].
- ²⁰L. A. Zaitseva and I. B. Levinson, Fiz. Tverd. Tela (Leningrad) **24**, 1286 (1982) [Sov. Phys. Solid State **24**, 731 (1982)].

Translated by A. Tybulewicz